Adhesion of perfume-filled microcapsules to model fabric surfaces

Journal Item

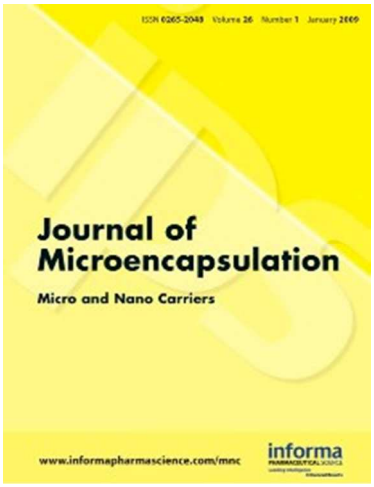

Adhesion of Perfume-Filled Microcapsules to Model Fabric Surfaces

Journal:	*Journal of Microencapsulation*
Manuscript ID:	TMNC-2013-0087
Manuscript Type:	Original Paper
Date Submitted by the Author:	21-May-2013
Complete List of Authors:	He, Yanping; University of Birmingham, Bowen, James; University of Birmingham, Andrews, James; University of Birmingham, Liu, Min; University of Birmingham, Smets, Johan; Procter & Gamble, Zhang, Zhibing; University of Birmingham, Sch Chem Engineerng
Keywords:	Chitosan, Microcapsules, Powder technology, Disposition, Physical characterisation, Surface modification

Adhesion of Perfume-Filled Microcapsules to Model Fabric Surfaces

Yanping He[1], James Bowen[1], James W Andrews[1], Min Liu[1], Johan Smets[2] and Zhibing Zhang[1]*

[1]School of Chemical Engineering, University of Birmingham, Edgbaston, Birmingham, B15 2TT, UK;

[2]Proctor & Gamble Brussels Innovation Center, Temselaan 100 1853 Strombeek Bever, Belgium

Corresponding author: Zhibing Zhang

*Email: z.zhang@bham.ac.uk

Phone: 44-121-4145334

Key terms:

Chitosan; cellulose thin film; flow chamber technique; atomic force microscopy; bridging force; electrostatic attraction.

ABSTRACT

The retention and adhesion of melamine formaldehyde microcapsules on a model fabric surface in aqueous solution were investigated using a customized flow chamber technique and atomic force microscopy (AFM). A cellulose film was employed as a model fabric surface. Modification of the cellulose with chitosan was found to increase the retention and adhesion of microcapsules on the model fabric surface. The AFM force-displacement data reveal that bridging forces resulting from the extension of cellulose chains dominate the adhesion between the microcapsule and unmodified cellulose film, whereas electrostatic attraction helps to adhere the microcapsule to the chitosan-modified cellulose film. The correlation between results obtained using these two complementary techniques suggests that the flow chamber device can be potentially used for rapid screening of the effect of chemical modification on the adhesion of microparticles to surfaces, reducing the time required to achieve an optimal formulation.

1. INTRODUCTION

Perfume-filled microcapsules have been developed to be used in detergent products, including washing powders (Brown and Bowman, 1985), liquid detergents (Broeckx et al., 2004) , bleach (Bianchetti et al., 2010), and personal cleaner (Ouali and Benczedi, 2008), to provide a long-lasting release of pleasant odour to consumers after cleaning. Perfume is a mixture of fragrant essential oils and aroma compounds, fixatives, and solvents used to give the human body, animals and objects a pleasant scent (Sell, 2006). For the former application, the microcapsules attach to the fabric surface and become entrained within the woven fabric structure during the laundry process and release perfume oil by diffusion through the

microcapsule wall or by rupture of the microcapsules via friction and rubbing with human body. Therefore, understanding the adhesion mechanisms of microcapsules to surfaces is of fundamental importance for maximizing their deposition onto fabrics.

The adhesion of microparticles and cells on substrates has previously been investigated using shear flow in a flow chamber (Sanjit et al., 1994, Garrett et al., 2008). The removal of particles from a surface through hydrodynamic forces (Decuzzi et al., 2007) can be adjusted by the choice of flow velocity and the consequently shear stress imposed upon the particles; it is the most common technique used to study adhesion of particles on a surface in liquid environments (Martines et al., 2004, Renshaw et al., 2005, Garrett et al., 2008). Microparticles exposed to shear flow are expected to be displaced by lift, sliding, rolling or some combination thereof (Saffman, 1965, Zhang et al., 1999a, Zoeteweij et al., 2009). Particles are removed by lift motion when the lift forces overcome the adhesion in direction normal to the surface (Zoeteweij et al., 2009). If the lift is not sufficient, particles can also be displaced by drag forces in the lateral direction through either sliding or rotating motion (Sanjit et al., 1994, Zhang et al., 1999a, Zoeteweij et al., 2009). The balance on the forces and torques resulting in particle removal from the surface is directly correlated with the adhesion between the two surfaces. Crucially, the technique provides adhesion information for a population of particles, providing statistically significant information in a short period of time.

In contrast, atomic force microscopy (AFM) can be used to measure micro- and nanoscale forces between a single particle and a surface of interest via a colloid probe technique (Binnig et al., 1986, Ducker et al., 1992, Kappl and Butt, 2002). A candidate particle is attached to the end of a microfabricated cantilever and the force between the particle and surface can be measured with AFM in different environments. AFM with a colloidal probe has been

successfully employed in many systems, including for measuring the interactions between a cellulose microparticle and a cellulose thin film (Notley, 2009), a silica sphere and a mica plate (Vakarelski et al., 2000, Vakarelski and Higashitani, 2001), and a melamine formaldehyde (MF) micro sphere and a cellulose thin film (Liu et al., 2013). Adhesion has been investigated either by comparison of adhesive forces on specimen with different chemical compositions (Eastman and Zhu, 1996, Żbik and Frost, 2010) and surface roughness (Cooper et al., 2001, Katainen et al., 2006), or through interpretation of the force-displacement data by varying relativity humidity, ionic strength, pH, hydrophobic or hydrophilic nature etc to explore adhesion mechanisms including capillary force (Jones et al., 2002), electrostatic interaction (Vakarelski et al., 2000), hydrophobic interaction (Żbik and Frost, 2010) and bridging interaction (Notley, 2009, Kocuna et al., 2011).

In this study, a custom-built flow chamber was employed in order to investigate the retention and removal of perfume-filled MF microcapsules from a model cellulose thin film. AFM measurements were also performed in order to obtain information regarding the specific interactions which occur between individual particles and the surface. The cellulose film was also modified with chitosan and the adhesion and removal of microcapsules on it were investigated. Finally, the adhesion between particle and surface in different aqueous environments was quantified by the two techniques in order to elucidate the possible adhesion mechanisms.

2. METHODS

2.1 Perfume-filled MF microcapsules

Perfume-filled MF microcapsules (supplied by Procter & Gamble, Belgium) were produced by in-situ polymerization of MF precondensate and formaldehyde with poly-(acrylamide-

acrylic acid, sodium salt) at a temperature range of 55-85 °C. The core oil which constitutes the centre of the microcapsule is a typical perfume blend of various components (Long et al., 2010), all of which have a relatively low solubility in water, and are used in consumer products. The mean diameter of the perfume microcapsules is 20.0 ± 0.3 μm, measured with a Malvern particle sizer (APA2000, Malvern Instruments Ltd., UK).

2.2 Cellulose thin film

2.2.1 Preparation

Cotton cellulose powder with a mean particle size of 20 μm (Sigma-Aldrich, UK) was used directly without any further purification. 50 wt% N-methylmorpholine-N-oxide (NMMO) solution (Sigma-Aldrich, UK) was used as received as a solvent to dissolve the cotton powder (Sigma-Aldrich, UK). Dimethyl sulfoxide (DMSO) (ACS spectrophotometric grade, ≥99.9 %, Sigma-Aldrich, UK) was used as a viscosity modifier. 50 % (w/v) poly(ethyleneimine) (PEI) in aqueous solution (Sigma-Aldrich, UK) was used as an anchoring polymer promoting adhesion of cellulose to the Si surface (single side polish Si wafers, 76 mm diameter, N <100>, resistivity 1-10 Ohm.cm, 381 μm thickness, IDB Technologies, UK). High Performance Liquid Chromatography (HPLC) grade H_2O (Fisher Scientific, UK) was used throughout. General purpose grade NaOH powder (Sigma-Aldrich, UK) was used to make 10 % (wt. %) NaOH solution. Detailed procedures describing the preparation of the cellulose thin film have previously been reported by Notley and Wågberg (2005) and Liu *et al.* (2013).

2.2.2 Preparation of chitosan-modified cellulose thin films

Chitosan (400 kg/mol; Sigma-Aldrich, UK) was dissolved into 10% (wt. %) acetic acid (Sigma-Aldrich, UK) solution and then diluted to 0.1%, 0.01% and 0.001% (wt. %) with

HPLC grade H_2O. 10% (wt. %) NaOH solution was used to adjust the chitosan solution to pH 6.

Flow chamber experiment: To modify the cellulose film, 0.1 mL of chitosan solution was injected to the flow chamber, full details of which are given in §2.3.1, using a cellulose film substrate of lateral dimensions 1.5 mm × 24 mm; the substrate dimensions were chosen to match the internal dimensions of the flow chamber. The solution and substrate were left in contact for 30 minutes. A continuous flow of H_2O at 10 mL/h was subsequently used to remove any unadsorbed chitosan and wash the chitosan-modified cellulose film for 5 minutes. A microcapsule suspension with a concentration of 0.5 % (wt. %) was injected to the flow chamber and the removal experiments were performed as described in §2.3.2.

AFM measurement: 140 μL of chitosan solution was deposited on a cellulose film of dimensions 10 mm × 10 mm and left in contact for 30 min, in order to maintain the same concentration of chitosan per unit area as used in the flow chamber experiment. The chitosan-modified cellulose film was then spun for 30 s at 1000 rpm using a spin processor (WS-400-6NPP, Laurell Technologies, USA). The chitosan-modified cellulose thin film was then immersed in HPLC H_2O for 5 min, before being used as the substrate in the AFM measurement.

2.3 Flow chamber experiments

2.3.1 Flow chamber device

A parallel-plate flow chamber was custom-built in order to measure the deposition and removal behaviour of a population of microcapsules on a cellulose film in an aqueous environment. The chamber consisted of a top plate, a gasket with a rectangular channel, a

cellulose film substrate, a piece of soft rubber, a bottom plate and suitable screws. Figure 1(a) shows a schematic of the flow chamber: (1) a rectangular transparent plastic plate (Poly(methyl methacrylate) (PMMA), 70 mm × 30 mm × 5 mm) with an entrance, outlet port and sample injection port; (2) a gasket (70 mm × 30 mm × 5 mm) with a rectangular channel (24 mm × 1.5 mm × 1.5 mm) as the main body of the flow chamber; (3) a piece of cellulose film with dimensions greater than those of the rectangular channel as the bottom substrate of the flow chamber; (4) a piece of soft rubber to ensure a well-defined seal between the cellulose film and the bottom plate; (5) a piece of transparent rectangular plastic plate (PMMA, 70 mm × 30 mm × 5 mm) as the bottom of plate. The flow chamber was fabricated by fixing the above pieces together with screws, which was then connected to a syringe pump (KD 100, KD Scientific Inc., USA) and a waste tank with rubber tubes, having an inner diameter of 2 mm. Figure 1(b) shows a schematic of the visualisation and measurement system.

2.3.3 Measurement of the deposition and removal of microcapsules in the flow chamber

HPLC H_2O was pumped through the system by ensuring no air bubble was present. 0.2 mL microcapsule suspension (0.5 wt. %) was then injected into the chamber through the sample injection port and these microcapsules were allowed to settle 10 min. Subsequently, the system was subjected to a flow of 0.1 mL/h for 5 min in order to remove any suspended free oil droplets introduced by occasional breakage of microcapsules and air bubbles imported by injection. A Navitar optical camera with an attached LED light source coupled with Leica QWin Pro V2.8 software (Leica Microsystems Imaging Solutions Ltd., UK) was used to capture the images of 6 positions in the flow chamber, as shown in Figure 2. Images of these six positions were recorded as the flow rate was increased, and continued to be taken until after removal of the microparticles deposited under these positions.

ImageJ (NIH, USA) was used to calculate the area occupied by microcapsules, A_t, for each region. The area of each recorded region is given by A_0. The quantity of microcapsules remaining on these areas was normalised, denoted by a_i, for each capture area i.

$$a_i = (A_t/A_0)_i \quad (1)$$

Where i= 1, 2, 3, 4, 5 and 6.

The mean normalised area is given by:

$$\overline{a_i} = \frac{\sum_{i=1}^{6} a_i}{6} \quad (2)$$

2.4 X-ray Photoelectron Spectroscopy (XPS)

X-ray Photoelectron Spectroscopy was used to analyse the composition of the surfaces before and after being modified by chitosan. The unmodified cellulose film was used as manufactured. The chitosan-modified cellulose film was prepared by applying 0.1% (wt.%) chitosan solution to an unmodified cellulose film for 30 min. In order to maintain the same concentration of chitosan per unit area, the same volume to area ratio was maintained as described in §2.2.2. Samples were gently washed with H_2O before drying under a stream of N_2. The cellulose films were analysed using a monochromated Al κα X-ray source (1486.6 eV) and the data acquired at normal emission with respect to the sample surface using a sampling spot size of diameter 1.2 mm. The analysis chamber base pressure was 2×10^{-11} mbar. The C 1s, O 1s, and N 1s photoelectron peaks were acquired using pass energy of 20 eV, which gave an energy resolution of 0.69 eV. The cellulose film is insulating and can become positively charged as electrons leave the sample surface. Therefore a flux of 1 eV electrons was used to compensate. Data were analysed using the CasaXPS package using Voigt lineshapes, a mixture of Gaussian and Lorentzian lines.

2.5 Zeta potential

A Zetasizer Nano Series (Malvern Instruments Ltd, UK) was employed for determining the zeta potential of perfume-filled microcapsules and chitosan in aqueous solution. Perfume-filled microcapsules were diluted using H_2O to a concentration of 0.1% (wt. %). Chitosan (400 kg/mol; Sigma-Aldrich, UK) was dissolved into 10% (wt. %) acetic acid, which was then diluted to a 0.01% (wt. %) solution. HCl and NaOH aqueous solutions were used to adjust pH. A series of 0.1% (wt. %) microcapsule suspensions and 0.01% (wt. %) chitosan solutions with pH values of 3, 5, 7, 9 and 11 were formulated. Then, the zeta potential was measured using three separate samples. Data were averaged in order to obtain a mean value for the zeta potential.

2.6 Atomic Force Microscopy

A NanoWizardII atomic force microscope with an attached CellHesion module (JPK Instruments, UK) was used for imaging cellulose films and measuring the adhesive properties between single microcapsules and the substrate of interest in H_2O. Imaging was performed in intermittent contact mode using a pyramidal-tipped Si cantilever (RTESP, Veeco, France) with a nominal spring constant of 40 N/m. Adhesive forces between single microcapsules and substrates were measured using tipless rectangular Si cantilevers (NSC12, MikroMasch, Estonia) with a 20 μm diameter microparticle attached at the cantilever free end using araldite instant clear glue (Araldite, UK). Single microcapsule was attached onto a tipless cantilever by the aid of a micromanipulation rig which was used for precise displacement control (Zhang et al., 1999b). The cantilever spring constant was calculated by measuring their width, length and resonant frequency according to the method described by Bowen *et al*. (Bowen et al., 2010).

Substrates were attached to a poly(styrene) Petri dish, of diameter 35 mm and height 4 mm, which was subsequently firmly secured on the AFM stage, and filled to at least 2 mm height with H_2O (HPLC grade, Fisher Scientific, UK), ensuring there was no air bubble present. Upon immersion of the cantilever in the H_2O, the system was left to thermally equilibrate for 10 min. A minimum of 25 measurements were performed over an area of 10 μm × 10 μm for each microcapsule. The particle/surface contact time was set to either 0.01 s or 10 s. The approach velocity was 20 μm/s and the setpoint compressive load was 10 nN. After each set of measurements, the cantilever with microcapsule was washed gently with H_2O to remove any possible contamination on the microcapsule surface.

The adhesive force between microcapsules and substrates were measured in 10^{-3} M, 10^{-2} M and 0.1M NaCl solution, and also in 10^{-3} M NaCl solution, the pH of which was adjusted within the range 3 to 11.

3 RESULTS

3.1 Modification of cellulose thin film with chitosan

Cellulose films were modified with chitosan in an attempt to enhance the adhesion of microcapsules on them. The surface properties of cellulose thin films before and after the modification were investigated by XPS and AFM to ensure that the modification was successful.

3.1.1 Surface composition

Cellulose is an organic compound with the formula of $(C_6H_{10}O_5)_n$ (Johansson and Campbell, 2004); while the formula of chitosan is $(C_6H_{11}O_4N)_n$ (Franca et al., 2011). Therefore, the N

1s photoelectron peak was used to indicate the adsorption of chitosan to the cellulose surface, because nitrogen is absent in cellulose but present in chitosan (Da Róz et al., 2010, Franca et al., 2011). Figure 3 shows the results of XPS analysis of both cellulose thin film and the chitosan-modified surface. The cellulose film does not display a N 1s photoelectron peak, found in the binding energy region 401 ± 5 eV. In contrast, the chitosan-modified cellulose film exhibits a clear peak in this region, indicating the successful adsorption of chitosan. Similar results of adsorption of chitosan onto model cellulose thin films through electrostatic attraction were observed by Da Róz *et al.* (2010) and Orelma *et al.* (2011) with XPS.

3.1.2 Surface topography

The surface topography of cellulose films was imaged using AFM. In Figure 4, the root mean square (RMS) roughness of a dry cellulose film measured over a scan area of 5 µm x 5 µm is 5.4 ± 0.4 nm. After modification by chitosan, the surface roughness increased to 9.2 ± 0.3 nm. The increase in surface roughness after modification was also observed in Da Róz *et al.*'s work (2010), in which the RMS roughness of cellulose films over a scan area of 2.5 µm x 2.5 µm was reported as 13 nm, which increased to 33 nm over a scan area of 5 µm x 5 µm after modification by chitosan. Therefore, the results presented here indicate that chitosan was attached to the cellulose film successfully.

3.2 Deposition and removal of microcapsules in the flow chamber device

3.2.1 Microcapsule distribution after removal

The removal of microcapsules from a cellulose film was investigated as a function of the distance from the entrance of the flow chamber (Figure 5). Microcapsules were evenly distributed before using the water flow (Figure 5(a)). After using a H_2O flow of 80 mL/h for 3 min, to attempt removal of microcapsules from the cellulose film, a significant number of

microcapsules were displaced from the cellulose film; more microcapsules were detached from the area near the entrance and exit than in the centre region of the chamber (Figure 5(b)). It is suggested that the turning type configuration of flow chamber is the main reason to cause the uneven distribution of velocity in the flow chamber (Bakker et al., 2003), in which the fluid velocity is found to be higher at the transition between the vertical inlet and outlet, and the parallel plate middle region.

3.2.2 Microcapsule deposition on modified cellulose thin film with chitosan

Figure 6 shows the results of three repeated experiments of the removal of microcapsules from a cellulose film and chitosan-modified cellulose film with a water flow of 80 mL/h, for different concentrations of chitosan solution. The shear stress was estimated to be 3.95×10^{-2} Pa, assuming the viscosity of water to be 10^{-3} Pa.s at 20 ^{o}C (Bakker et al. 2003). The modification of the cellulose film by chitosan promoted significant particle retention. For chitosan solutions of concentration 0.01% and 0.1%, the retention of the microcapsules after exposure to the water flow for 3 min is in excess of 90 %.

The removal of microcapsules adhered to a surface in a flow chamber device is a dynamic process. The displacement of microparticles from surface was conventionally suggested to be via rotation (Sanjit et al., 1994, Zhang et al., 1999a, Zhang, 1999, Zoeteweij et al., 2009). Modification of the cellulose film with chitosan altered the surface chemical moieties available for interaction with adhering species; furthermore the surface roughness was also altered. Chitosan is cationic under the aqueous conditions employed here, and may adsorb to the anionic cellulose film through electrostatic attraction (Da Róz et al., 2010). The resultant adhesion between anionic MF microcapsules and the modified surfaces may be increased through electrostatic attraction and bridging forces (Fras Zemljic□ et al., 2009, Da Róz et al.,

2010). With increasing chitosan concentration on the cellulose film there may be a greater polycationic surface charge, which increased the adhesion of MF microcapsules. Correspondingly, a greater shear stress was required in order to displace the adhered microparticles. Therefore, under conditions of constant shear stress but increasing chitosan concentration, a greater number of MF microcapsules remained adhered to the modified cellulose film.

3.3 Adhesion measured with AFM

Figure 7 presents typical force-displacement data for the interaction between a single MF microcapsule and an unmodified cellulose film in HPLC H_2O. From point A to B the microcapsule approached the cellulose film and the only force acting on the cantilever was hydrodynamic resistance, which is negligible. At point B an out-of-contact repulsive force occurred between the two surfaces, followed by close approach of the microcapsule to the surface; under immersed conditions there might or might not be intimate contact of the MF microcapsule and cellulose film, due to hydration of the surfaces by H_2O molecules (Vakarelski et al., 2000). From B to C there is an increasing compressive load applied to the cantilever as the fixed end was moved more closely to the cellulose film; when the compressive load reached the setpoint value at point C the fixed end began to retract and the compressive load began to decrease. This continues to occur until point D, which is the position of the maximum adhesive force between the MF microcapsule and cellulose film. The cantilever was under a tensile load at this point. At point E the cantilever deflection was restored to the initial position, similar to the out-of-contact approach deflection recovered to zero position and then departed from the substrate. In Figure 7, there is no obvious “snap –in” on the approach curve when the microcapsule approached the cellulose film. Normally, the

attractive interaction during the approach process will promote particle adhesion to a surface; the stronger the attraction, the greater the retention of particles (Hilal and Bowen, 2002).

The mean maximum adhesive force between 5 single MF microcapsules and a cellulose film before and after modification by chitosan are shown in Figure 8. Both the adhesion between microcapsules and the cellulose thin film with a short contact time (0.01 s) and a longer contact time (10 s) were measured. The mean maximum adhesive force between a single MF microcapsule and the unmodified cellulose film is 2.3±1.0 nN for a contact time of 0.01s, which increases to 57.7±31.1 nN after modification using chitosan with a concentration solution of 0.1 % (wt. %). The large standard error may be attributed to the small number of MF microcapsules investigated and the difference in the surface properties between microcapsules, in which the surface asperities appear to be the main reason to cause the variation of adhesion, following suggestions of Hodges et al. (2004) AND Katainen et al., (2006) on similar systems. The adhesion was also found to increase when the contact time was increased from 0.01 s to 10 s, which is consistent with the results reported for adhesion between a PCL-grafted cellulose sphere and a neat cellulose sphere (Nordgren et al., 2009). When the two surfaces were brought together, molecular chains on the surfaces might start to extend and then entangle with each other, leading to an increase of the pull-off force when separated (Poptoshev and Claesson, 2002, Nordgren et al., 2009). The adhesion results from AFM validate the flow chamber data that modification of the cellulose film with chitosan enhanced adhesion between the MF microcapsules and the cellulose film, and also that the adhesion increased with increasing chitosan concentration, resulting in greater retention of MF microcapsules on the substrate in the flow chamber.

4 DISCUSSION

The results from both the flow chamber experiments and AFM measurements indicate that chitosan enhanced the interaction between the MF microcapsules and the cellulose film. In order to understand the possible mechanisms, the Zeta potential of the MF microcapsules in aqueous suspension was measured and their adhesion on a cellulose film exposed to different pH and ionic strength was further investigated.

4.1 Zeta potential

The Zeta potential of MF microcapsules in aqueous suspension and chitosan in solution are shown in Figure 9. MF microcapsules were negatively charged over a pH range of 3 to 11, which correlates with the results obtained by Liu (2010). Chitosan is a positive polysaccharide containing D-glucosamine groups (Che et al., 2008), and they will be protonated under low pH environment, leading to a high surface charge; amino group will become deprotonated with increasing pH and the surface charge becomes increasingly lower.

4.2 Adhesion as a function of ionic strength

The interaction between single microcapsules and a cellulose thin film before and after modification with chitosan was measured as a function of ionic strength of NaCl solution by AFM, and the data are shown in Figure 10. The repulsive interactions can be observed when the microcapsule approached a cellulose thin film in HPLC water (Figure 10 (a)), and the increase of ionic concentration decreases the decay length (Israelachvili, 2011). The repulsion force might originate from electrostatic repulsion because both MF microcapsules and the cellulose film are negatively charged (Liu, 2010). The increase of the ionic strength decreases the thickness of the electrical double layer (Zoppe et al., 2011), which decreases the decay length. After the two surfaces contacted, adhesion was detected on separation (Figure 10 (b)). However, no significant adhesion was observed between single MF microspheres and a

cotton film on separation in Liu *et al.*'s work (2013). The inconsistency may be attributed to the difference in chemical composition of MF microcapsules and microspheres. The MF microspheres are solid spheres made of pure MF without any surfactant (Liu et al., 2013). However, in addition to pure MF, acryl amide/acrylic acid copolymer is another component added to produce MF microcapsules (Long et al., 2010, Pan et al., 2012). The copolymer contains amine and carboxyl groups, which favour to form hydrogen bonding with carboxyl and hydroxyl groups on cellulose film respectively (Douglas et al., 2008).

Furthermore, 25 approach curves were analysed. Among them, 11 curves show the "snap-in" valleys on approach for NaCl solution of 10^{-3} M and 10^{-2} M as presented in Figure 10(a). This is possibly because of the loose extension of cellulose chains causing steric hindrance (Notley, 2009) in the solution with low ionic concentration. When the microcapsule approached the surface, it probably met the loose cellulose chains at first. Then a repulsive force was generated from compressing cellulose chains. Whenever a group of cellulose chains were compressed, a "snap-in" event was produced. The difference in the effective length of the cellulose chain might be the main reason to cause several "snap-in" valleys. However, in a solution with a high ionic concentration, the cellulose chains were folded and compressed into a dense layer (Zoppe et al., 2011). Therefore, no multiple "snap-in" events were detected as shown in Figure 10(a). Figure 11 presents a schematic of the interaction between a microcapsule and cellulose chains in a solution with different ionic concentrations.

The extension of cellulose molecule chains to the surface of microcapsules can also be explained by the detailed information on separation: in a weak ionic environment, the microcapsule separated from the cellulose surface with plateau events before the force dropped to zero for NaCl solution of 10^{-3} M in Figure 10 (b); while in an environment with

high ionic strength, a sharp pop-up interaction before the microcapsule was really separated with the surface was observed because cellulose chains were folded (Notley, 2009, Zoppe et al., 2011) and the microcapsule might meet a pop-up with the folded cellulose chains before final separation with the attached extended cellulose chains. 25 retract curves were analysed and 16 cases exhibited obvious sharp pop-up interaction in 0.1 M NaCl solution as shown in Figure 10 (b), which means it is not an occasional case. Therefore, the bridging force is considered to be the main mechanism of the adhesion in this case. The bridging interaction proposed here is consistent with Zoppe *et al.*'s work (2011) when they investigated the surface interaction between a silicon sphere probe and a cellulose nanocrystal surface modified with poly (NiPAAm) as brushes.

After the cellulose film was treated with chitosan, the attractive forces were observed on approach (Figure 10 (c)), which is in direct contrast to comparable measurements with the unmodified cellulose film in Figure 10 (a). After the modification, the microcapsule and cellulose film surfaces had opposite charges. When a microcapsule approached the modified surface, electrostatic attraction occurred to capture the microcapsule to the surface, enhancing the adhesion. Therefore the increase of ionic strength screening the attractive interaction between the two surfaces was observed in NaCl solution of 0.1 M, see Figure 10 (d). The plateau force-separation shape is observed on retraction and the tip-surface separation distance is about 1000 nm (Figure 10 (d)). It is about 5 to 10 times of chitosan contour length (94 to 178 nm) measured in Kocuna *et al.*'s work (2011) when they studied the contour length of single chitosan molecules. It should be mentioned that the chitosan molecule used in this work (400, 000 g/Mol) is about twice as big as the one used in Kocuna *et al.*'s work (220, 000 g/Mol); and also the diameter of the microcapsule probe is much bigger than that of a tip on a cantilever, so there were more chitosan strands (Kocuna et al., 2011) attaching on

the microcapsule surface, extending the tip-surface separation distance. Therefore, after contact positively charged chitosan acts as a "polyelectrolyte bridge" and "molecule chain bridge" connecting the negatively charged microcapsule and negatively charged cellulose thin film. When two surfaces were separated, a higher force was needed.

4.3 Adhesion as a function of pH

The adhesion between MF microcapsules and an unmodified cellulose film decreased with increasing pH of the suspension liquid, as shown in Figure 12(a). However, the adhesion between microcapsules and the modified cellulose film firstly increased and then decreased with pH (Figure 12 (b)). The maximum value is observed at pH 5. Both non-modified cellulose film and MF microcapsules are negatively charged and their surfaces become more negative by increasing the pH, causing the decrease of adhesion between them. However, after chitosan molecules were attached on the cellulose film, amine groups of chitosan are totally protonated and deprotonated at pH 3 and pH 11 respectively. At pH 3 or pH 11, the carboxyl groups (Liu, 2010) on the surface of the microcapsules are uncharged or negatively charged. So the attraction is weak between them. Both functional groups on the surface of microcapsule and modified cellulose surfaces are of half-deprotonation in medium pH range (The pK_a value of charged carboxyl group on cellulose and glucosamine segments on chitosan molecule is 4-5 (Notley, 2009) and 6.3-7.5 (Claesson and Ninhami, 1992, Kocuna et al., 2011) respectively. Therefore, the attraction between the microcapsule and modified surface reached a maximum value under pH 5. Besides electrostatic attraction at the medium pH, amine groups and carboxyl groups on two surfaces may form hydrogen bonding (Giesbersa et al., 2002), which helps to promote the adhesion. Additionally, a shape of the plateau in the force -separation curve is observed in low pH environment (Figure 12 (a)). In low pH solution, the carboxyl group on cellulose molecule is fully protonated. Cellulose film

under this condition extended into solution loosely, causing the plateau events on retraction (Notley, 2009). Therefore, the bridging force, because of the extension of cellulose chains, dominated the interaction between the microcapsule and cellulose thin film. However, the interaction between the microcapsule and chitosan-modified surface is mainly due to electrostatic attraction on approach. The strong electrostatic attraction brings the two surfaces into close contact and there will be charge neutralization on approach. Upon separation, extra force will be required (Giesbersa et al., 2002). Additionally, hydrogen bonding and chitosan molecules act as bridges (Kocuna et al., 2011) increasing the energy required to separate the two surfaces, which corresponds to an increase in the peak force on separation.

5 CONCLUSIONS

Chitosan was successfully introduced to the surface of a cellulose thin film and the retention of perfume-filled melamine formaldehyde microcapsules on the cellulose film was correspondingly enhanced. The surface area covered by deposited microcapsules increased from about 10 % to 90 % at a shear stress of 3.95×10^{-2} Pa before and after chitosan solution with a concentration of 0.1 % (wt) was applied to a cellulose thin film for 30 min. Correspondingly, the average pull-off force between single microcapsules and the cellulose thin film increased from 2.3 ± 1.0 nN to 57.7 ± 31.1 nN, as measured by AFM with a contact time of 0.01 s. The agreement between the adhesion results obtained using the two techniques indicates that the flow chamber device can be potentially used as a tool for fast screening the effects of various chemicals on the adhesion of microcapsules on different fabric surfaces.

The mechanism of adhesion between the microcapsule and unmodified cellulose thin film was mainly attributed to the bridging force resulting from the extension of cellulose molecule

chains. After the modification, chitosan molecules attached on the surface of the cellulose to capture microcapsules through electrostatic attraction and then the adhesion was enhanced by electrostatic attraction, bridging interaction and hydrogen bonding on separation.

Declaration of interest: The authors report no conflicts of interest.

Acknowledgement: The work was supported by Proctor & Gamble, Belgium and School of Chemical Engineering, University of Birmingham. The author (YPH) would like to thank China Scholarship Council for providing a stipend for her to study in UK, Dr Artur Majewski for technical support to build the flow chamber device. The AFM used in this research was obtained through Birmingham Science City: Innovative Uses for Advanced Materials in the Modern World (West Midlands Centre for Advanced Materials Project 2), with support from Advantage West Midlands (AWM) and partly funded by the European Regional Development Fund (ERDF).

References

Bakker DP, van der Plaats A, Verkerke GJ, Busscher HJ, Mei HC, 2003. Comparison of velocity profiles for different flow chamber designs used in studies of microbial adhesion to Surfaces. Appl Environ Microb 69**:** 6280-6287.

Bianchetti G, Ottavia E, Francois T, Smets J, Grande G, 2010. Bleaching compositions containing perfume microcapsules. US 20100180386.

Binnig G, Quate CF, Gerber C, 1986. Atomic force microscope. Phys Rev Lett 56**:** 930–933.

Bowen J, Cheneler D, Walliman D, Arkless SG, Zhang Z, Clward M, Adams MJ, 2010. On the calibration of rectangular atomic force microscope cantilevers modified by particle attachment and lamination. Meas Sci Technol 21**:** 106-115.

Broeckx W, August M, Del V, Eva M, 2004. Microcapsules. US 7897555.

Brown RW, Bowman RP, 1985. Capsule manufacture. US 4552811.

Che AF, Liu ZM, Huang XJ, Wang ZG, Xu ZK, 2008. Chitosan-modified poly(acrylonitrile-co-acrylic acid) nanofibrous membranes for the immobilization of concanavalin A. Biomacromolecules 9**:** 3397-3403.

Claesson PM, Ninhami BW, 1992. pH-dependent interactions between adsorbed chitosan layers. Langmuir 8**:** 1406-1412.

Cooper K, Gupta A, Beaudoin S, 2001. Simulation of the adhesion of particles to surfaces. J Colloid Interface Sci 234**:** 284-292.

da Róz AL, Leite FL, Pereiro LV, Nascente PAP, Zucolotto V, Oliveira JRON, Carvalho AJF, 2010. Adsorption of chitosan on spin-coated cellulose films. Carbohyd Polym 80**:** 65–70.

Decuzzi P, Gentile F, Granaldi A, Curcio A, Causa F, Indolfi C, Netti P, Ferrari M, 2007. Flow chamber analysis of size effects in the adhesion of spherical particles. Int J Nanomedicine 2: 689-696.

Douglas JG, Gloria SO, Ryan M, 2008. Adhesion and surface issues in cellulose and nanocellulose. J. Adhes Sci Technol 22**:** 545-567.

Ducker WA, Senden TJ, Pashley RM, 1992. Measurement of forces in liquid using a force microscope. Langmuir 8**:** 1831-1836.

Eastman T, Zhu DM, 1996. Adhesion forces between surface-modified AFM tips and a mica surface. Langmuir 12**:** 2859-2862.

Franca EF, Freitas LCG, Lins RD, 2011. Chitosan molecular structure as a function of N-acetylation. Biopolymers 95**:** 448-460.

fras Zemljic L, Pers in Z., Stenius P, 2009. Improvement of chitosan adsorption onto cellulosic fabrics by plasma treatment. Biomacromolecules 10**:** 1181-1187.

Garrett TR, Bhakoo M, Zhang Z, 2008. Characterisation of bacterial adhesion and removal in a flow chamber by micromanipulation measurements. Biotechnol Lett 30**:** 427-433.

Giesbersa M, Kleijnb JM, Stuarta MAC, 2002. Interactions between acid- and base-functionalized surfaces. J Colloid Interface Sci 252**:** 138-148.

Hilal N, Bowen WR, 2002. Atomic force microscope study of the rejection of colloids by membrane pores. Desalination 150**:** 289–296.

Hodges CS, Looi L, Cleaver JAS, Ghadiri M, 2004. Use of the JKR model for calculating adhesion between rough surfaces. Langmuir 20**:** 9571–9576.

Israelachvili JN, 2011. Intermolecular and surface forces. Oxford: Academic press.

Johansson L-S, Campbell JM, 2004. Reproducible XPS on biopolymers: cellulose studies. Surf Interface Anal 36**:** 1018-1022.

Jones R, Pollock HM, Cleaver JAS, Hodges CS, 2002. Adhesion forces between glass and silicon surfaces in air studied by AFM: effects of relative humidity, particle size, roughness, and surface treatment. Langmuir 18**:** 8045-8055.

Kappl M, Butt HJ, 2002. The colloidal probe technique and its application to adhesion force measurements. Part Part Syst Charact 19**:** 129-143.

Katainen J, Paajanen M, Ahtola E, Pore V, Lahtinen J, 2006. Adhesion as an interplay between particle size and surface roughness. J Colloid Interface Sci 304**:** 524–529.

Kocuna M, Grandboisb M, Cuccia LA, 2011. Single molecule atomic force microscopy and force spectroscopy of chitosan. Colloids Surf B Biointerfaces 82**:** 470-476.

Liu KM, Preece J, York D, Bowen J, Zhang Z, 2013. Measurement of the adhesion between single melamine formaldehyde resin micro-particles and a flat fabric surface using AFM. J Adhes Sci Technol, accepted

Liu M, 2010. Understanding the mechanical strength of microcapsules and their adhesion on fabric surfaces. PhD Thesis.

Long Y, Vincent B, York D, Zhang Z, Preece JA, 2010. Organic–inorganic double shell composite microcapsules. Chem Commun 46**:** 1718-1720.

Martines E, Mcghee K, Wilkinson C, Curtis ASG, 2004. A parallel-plate flow chamber to study initial cell adhesion on a nanofeatured surface. IEEE Trans Nanobioscience 3**:** 90-95.

Nordgren N, Lo¨nnberg H, Hult A, Malmstrom E, Rutland MW, 2009. Adhesion dynamics for cellulose nanocomposites. ACS Appl Mater Interfaces 1**:** 2098-2103.

Notley SM, 2009. Stretching and solvency of charged cellulose chains. ACS Appl Mater Interfaces 1**:** 1218-1223.

Ouali L, Benczedi D, 2008. Polyurethane and polyurea microcapsules. US 20080206291.
Pan X, York D, Preece JA, Zhang Z, 2012. Size and strength distributions of melamine-formaldehyde microcapsules prepared by membrane emulsification. Powder Technol 227**:** 43-50.
Poptoshev E, Claesson PM, 2002. Forces between glass surfaces in aqueous polyethylenimine solutions. Langmuir 18**:** 2590-2594.
Renshaw KM, Orr DE, Burg KJL, 2005. Design and evaluation of a novel flow chamber for measuring cell adhesion to absorbable polymer films. Biotechnol Prog 21**:** 538-545.
Saffman PG, 1965. The lift on a small sphere in a slow shear flow. J Fluid Mech. 22**:** 385-400.
Sanjit KD, Sharma MM, Schechter RS, 1994. Adhesion and hydrodynamic removal of colloid particles from surfaces. J Colloid Interface Sci 164**:** 63-77.
Sell CS, 2006. The Chemistry of Fragrances: From Perfumer to Consumer. London: The Royal Society of Chemistry.
Vakarelski IU, Higashitani K, 2001. Dynamic features of short-range interaction force and adhesion in solutions. J Colloid Interface Sci 242**:** 110-120.
Vakarelski IU, Ishimura K, Higashitani K, 2000. Adhesion between silica particle and mica surfaces in water and electrolyte solutions. J Colloid Interface Sci 227**:** 111-118.
Żbik MS, Frost RL, 2010. AFM study of forces between silicon oil and hydrophobic–hydrophilic surfaces in aqueous solutions. J Colloid Interface Sci 349**:** 492-497.
Zhang F, 1999. Submicron particle removal in post chemical mechanical planarization (CMP) cleaning. J Appl Phys A69**:** 437–440.
Zhang F, Busnaina AA, Feng J, Fury MA, 1999a. Particle adhesion and removal in chemical mechanical polishing (CMP) and post-CMP cleaning. J Electrochem Soc 146**:** 2665-2690.
Zhang Z, Saunders R, Thomas CR, 1999b. Mechanical strength of single microcapsules determined by a novel micromanipulation technique. J Microencapsul 16**:** 117-124.
Zoeteweij ML, Donck JCJVD, Versluis R, 2009. Particle removal in linear shear flow: model prediction and experimental validation. J Adhes Sci Technol 23**:** 899–911.
Zoppe JO, Osterberg M, Venditti RA, Laine J, Rojas OJ, 2011. Surface interaction forces of cellulose nanocrystals grafted with thermoresponsive polymer brushes. Biomacromolecules 12**:** 2788–2796.

Figure Captions

Figure 1 Design of a flow chamber (a) and schematic diagram of the flow chamber system (b)

Figure 2 The regions of the microchannel which were recorded, highlighted in shaded area. x represents the distance from the entrance and i sequence of recorded regions.

Figure 3 XPS analysis of cellulose thin film (a) and cellulose modified with 0.1% (wt. %) chitosan solution (b).

Figure 4 AFM images of dry cellulose thin film (5 μm ×5 μm) made of 0.5% (w/w) cotton powder (a); after modification with 0.1% chitosan (b) (RMS: (a) 5.4 ± 0.4 nm, (b) 9. 2± 0.3 nm)

Figure 5 Distribution of microcapsules as a function of the distance from the chamber entrance, before (a) and after (b) removal with a water flow of 80 mL/h for 3 min.

Figure 6 Effect of modification of cellulose film with chitosan on the removal of microcapsules. The error bar represents the standard error of three repeat measurements.

Figure 7 Schematic representation of interactions between a MF microcapsule with a diameter of 22.0 μm and a non- modified cellulose thin film in HPLC water.

Figure 8 Mean adhesion between 5 microcapsules and a cellulose thin film before and after being modified with chitosan solution. The error bar represents the standard error of the mean.

Figure 9 Zeta potential of MF microcapsules in aqueous suspension and aqueous chitosan solution with pH 3-11.

Figure 10 Typical force curves when single microcapsules interacted with the cellulose thin film ((a) approaching, (b) retracting) and modified cellulose thin film ((c) approaching, (d) retracting) in NaCl solution with different concentrations.

Figure 11 Schematic diagrams illustrating the configuration of cellulose molecule chains in different ionic concentration.

Figure 12 Typical force curves when the microcapsule was separated from the cellulose thin film before being modified (a) and after with chitosan (b), which were exposed to 10^{-3} M NaCl solution with different pH.

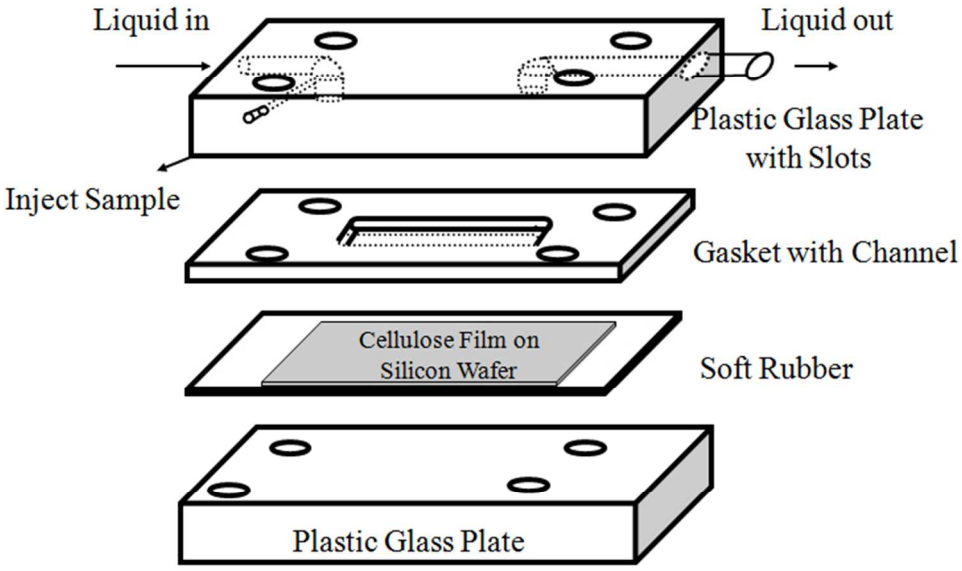

Fig 1(a)
200x124mm (96 x 96 DPI)

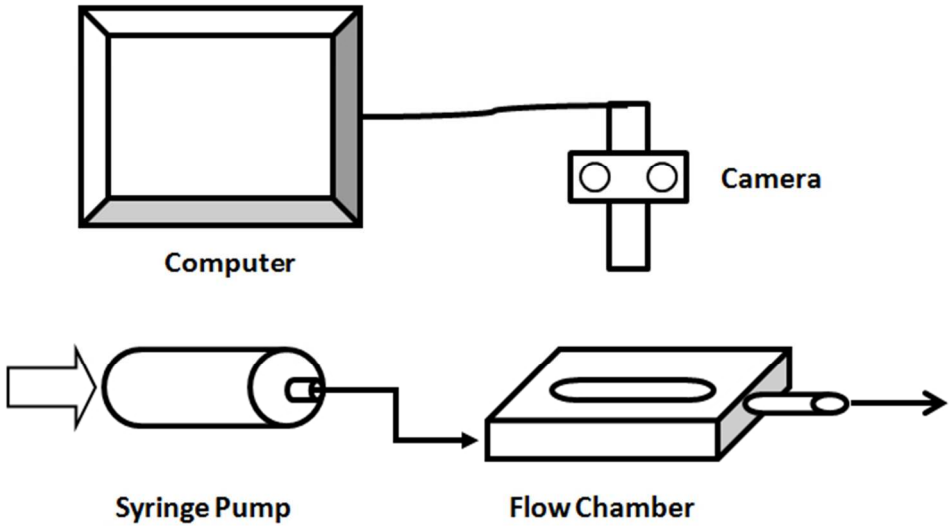

Fig 1(b)
185x110mm (96 x 96 DPI)

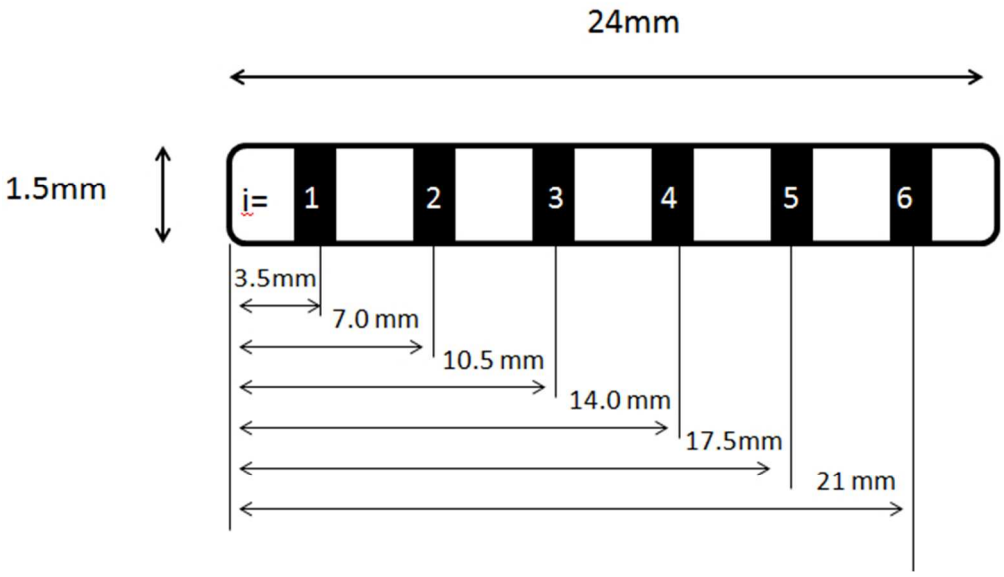

Fig 2
175x101mm (96 x 96 DPI)

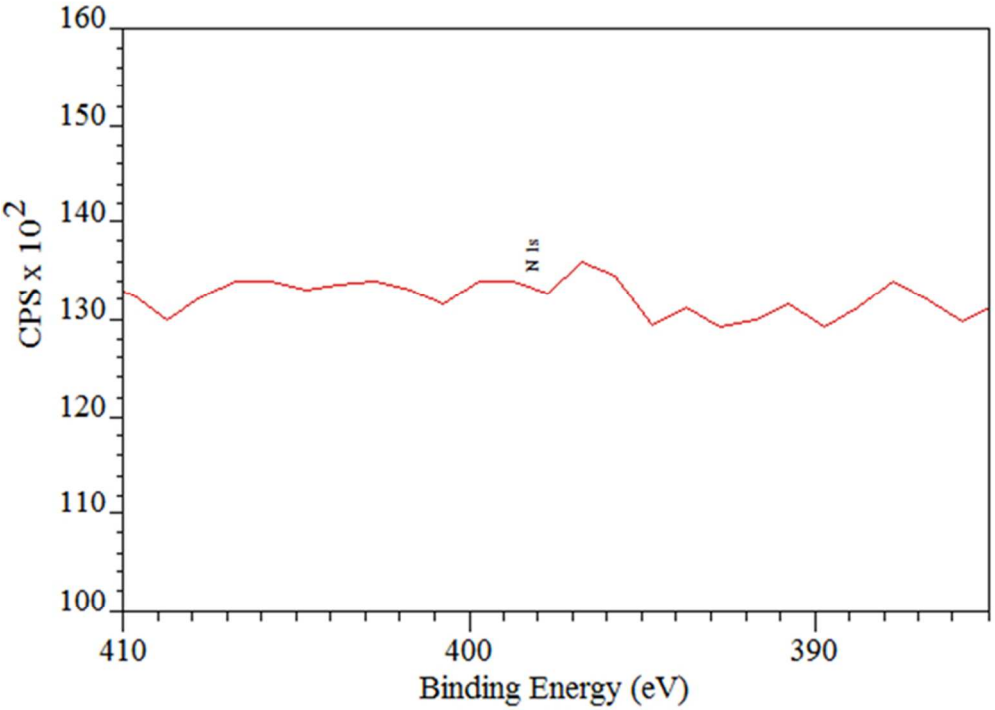

Fig 3(a)
203x148mm (96 x 96 DPI)

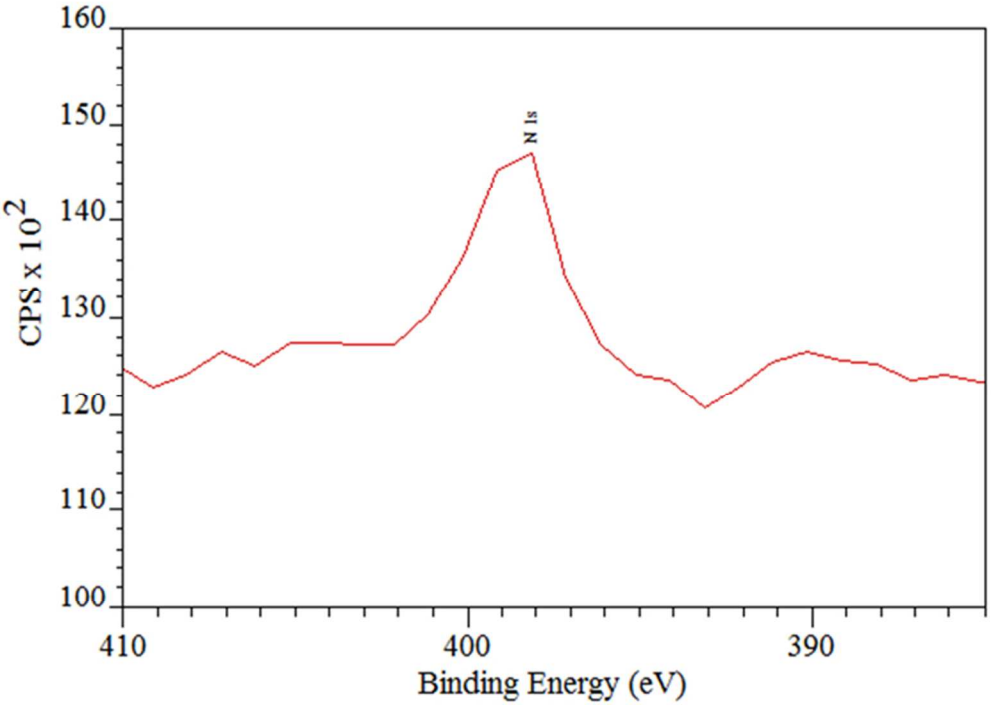

Fig 3(b)
205x148mm (96 x 96 DPI)

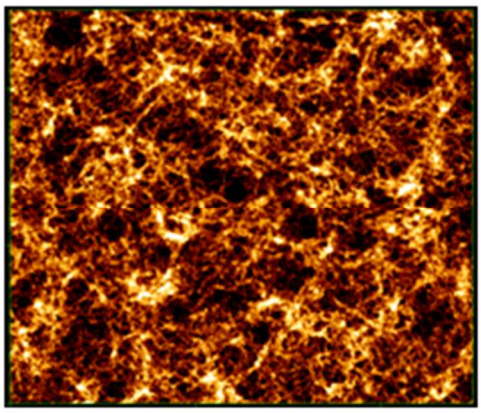

Fig 4(a)
63x53mm (96 x 96 DPI)

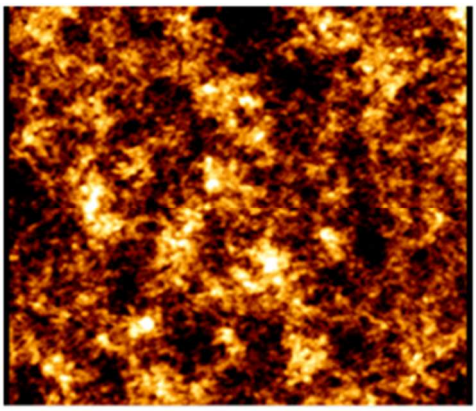

Fig 4(b)
62x53mm (96 x 96 DPI)

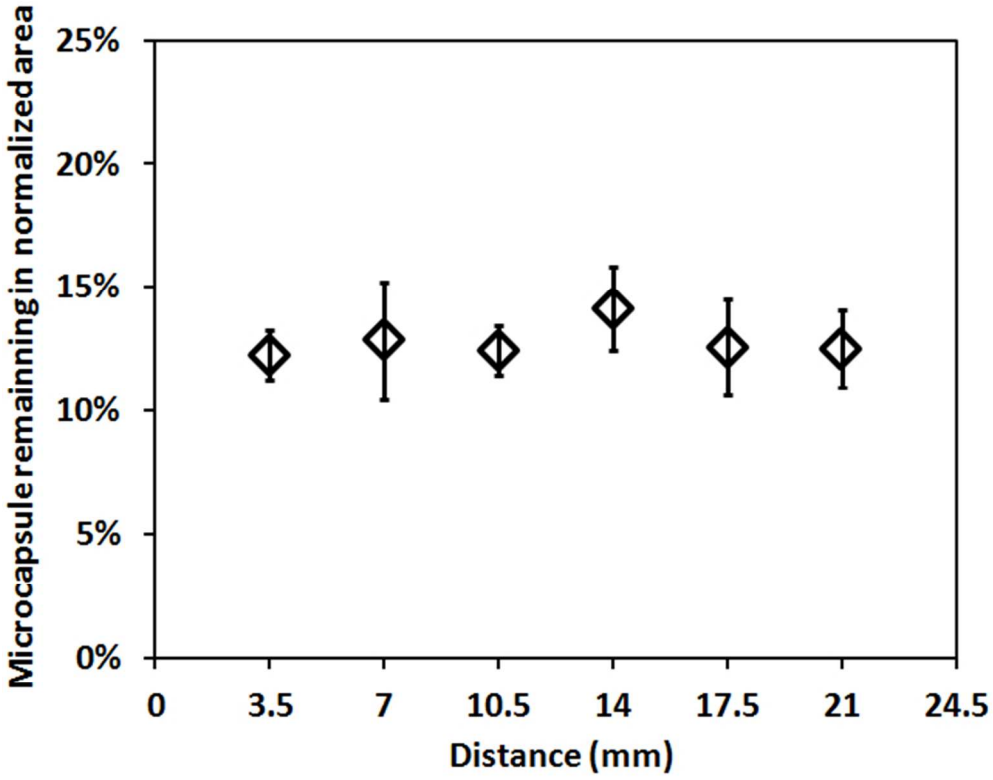

Fig 5(a)
171x133mm (96 x 96 DPI)

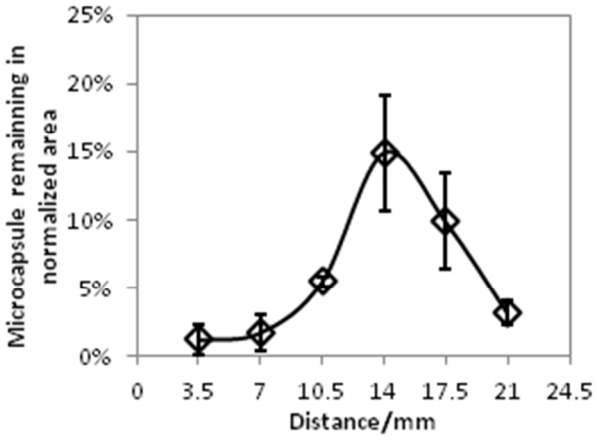

Fig 5(b)
82x61mm (96 x 96 DPI)

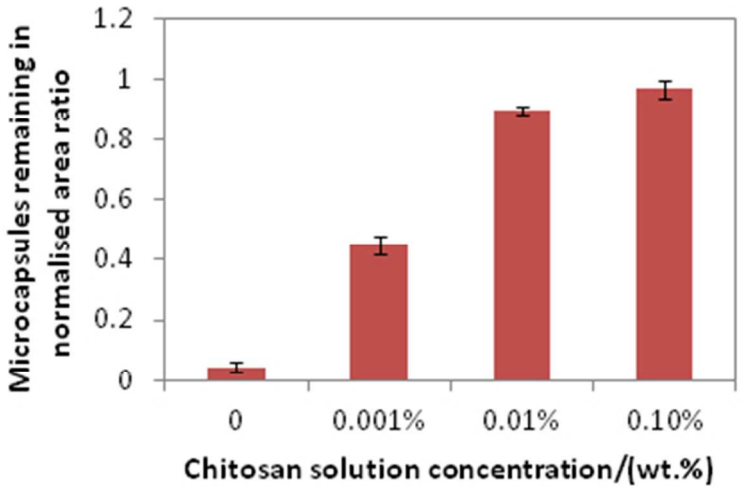

Fig 6
106x67mm (96 x 96 DPI)

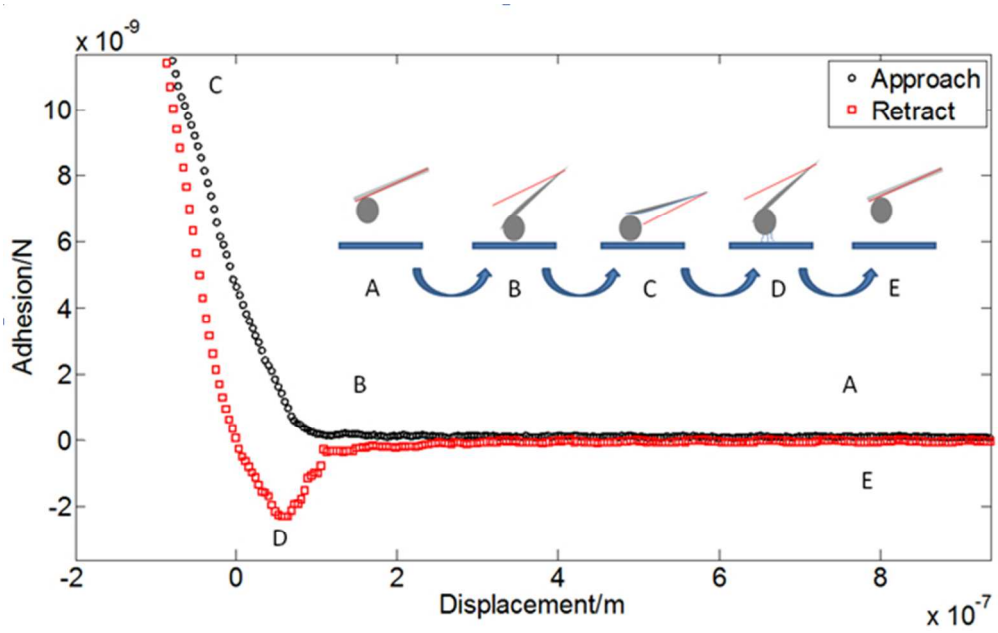

Fig 7
173x109mm (96 x 96 DPI)

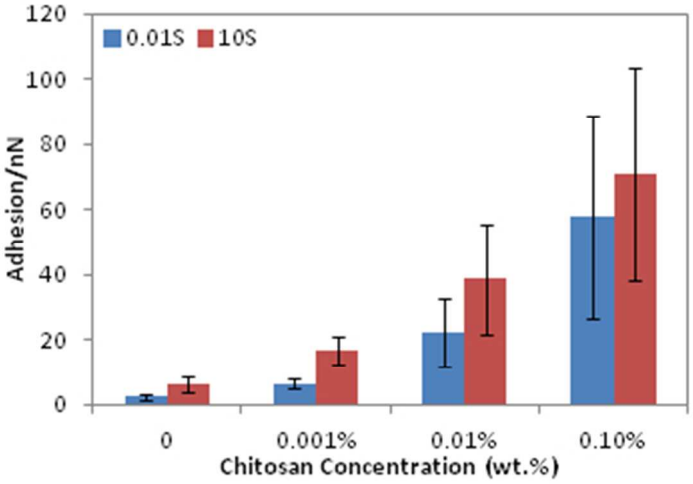

Fig 8
93x65mm (96 x 96 DPI)

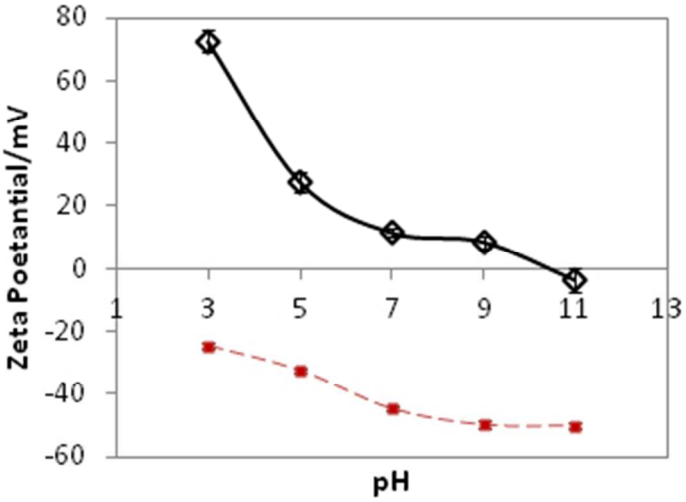

Fig 9
104x69mm (96 x 96 DPI)

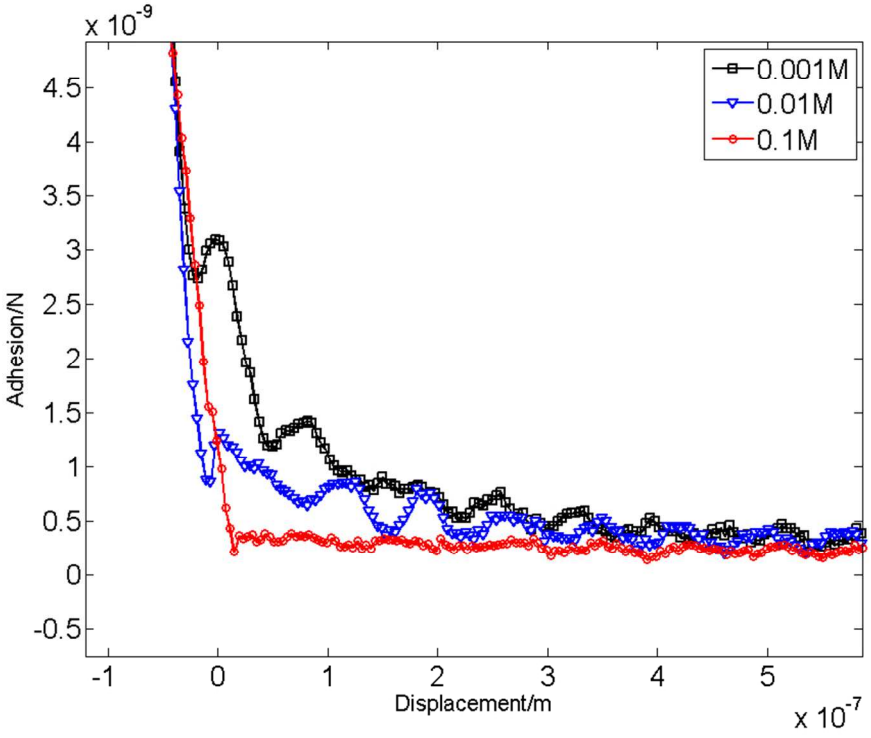

Fig 10(a)
259x196mm (96 x 96 DPI)

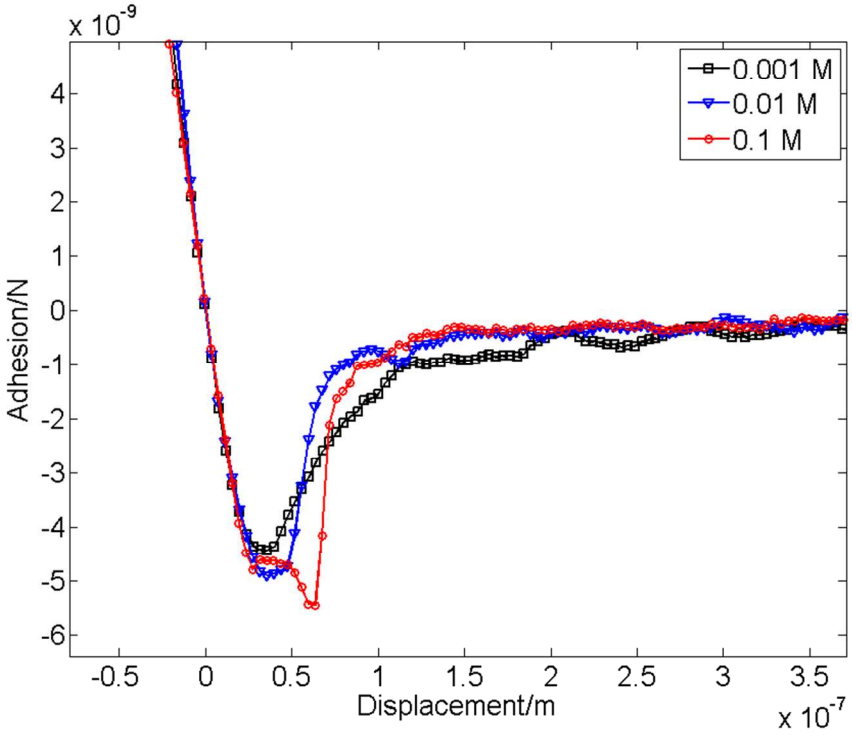

Fig 10(b)
259x196mm (96 x 96 DPI)

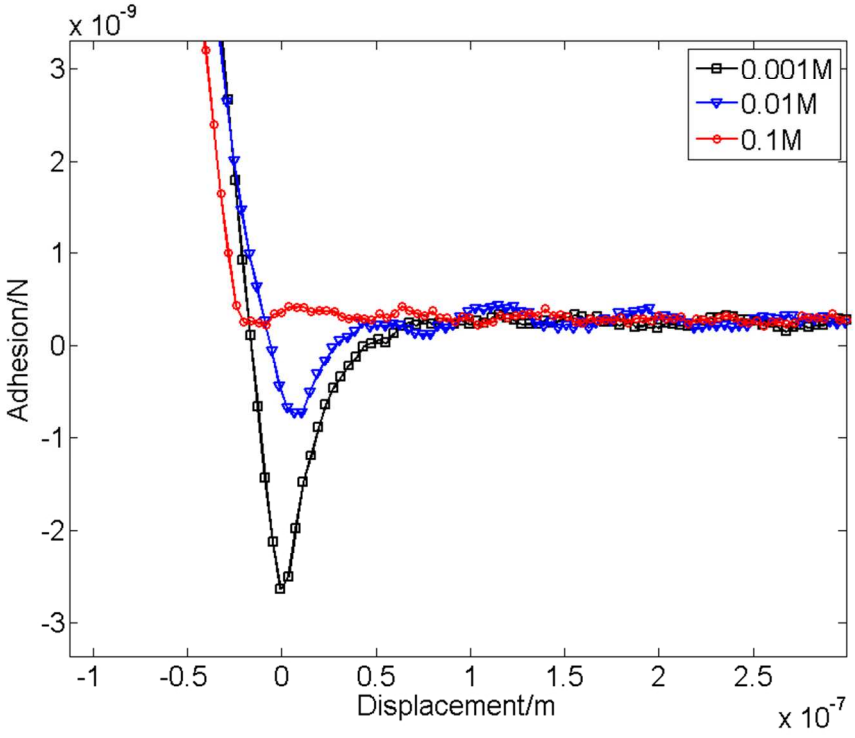

Fig 10(c)
259x196mm (96 x 96 DPI)

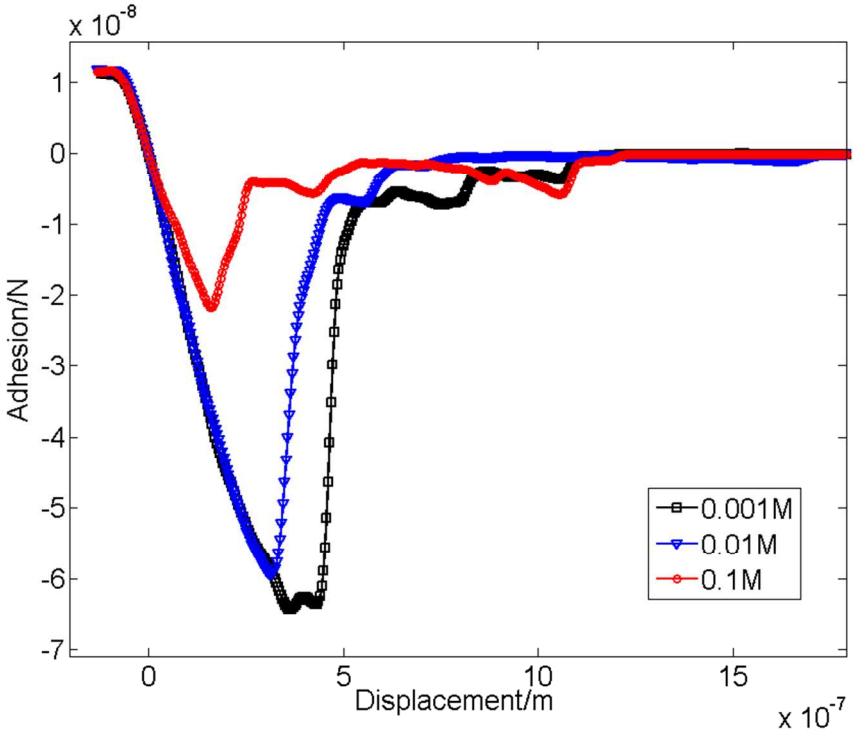

Fig 10(d)
259x196mm (96 x 96 DPI)

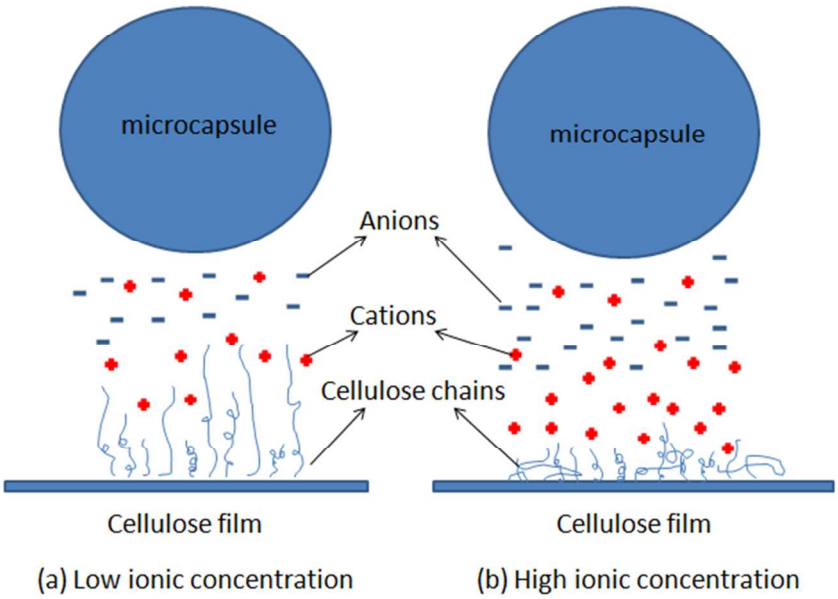

Fig 11
192x139mm (96 x 96 DPI)

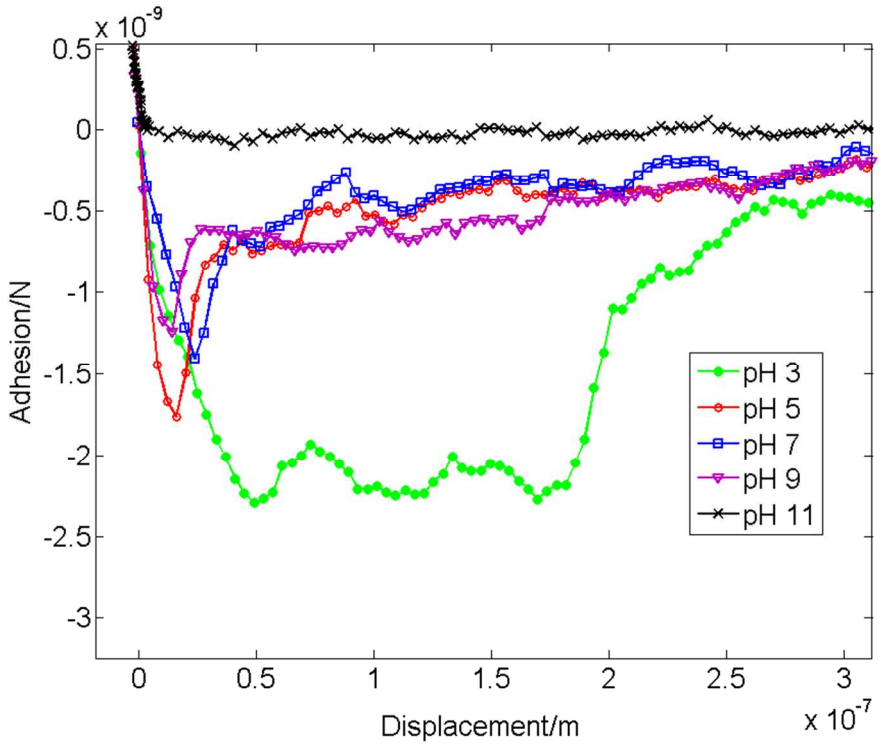

Fig 12(a)
259x196mm (96 x 96 DPI)

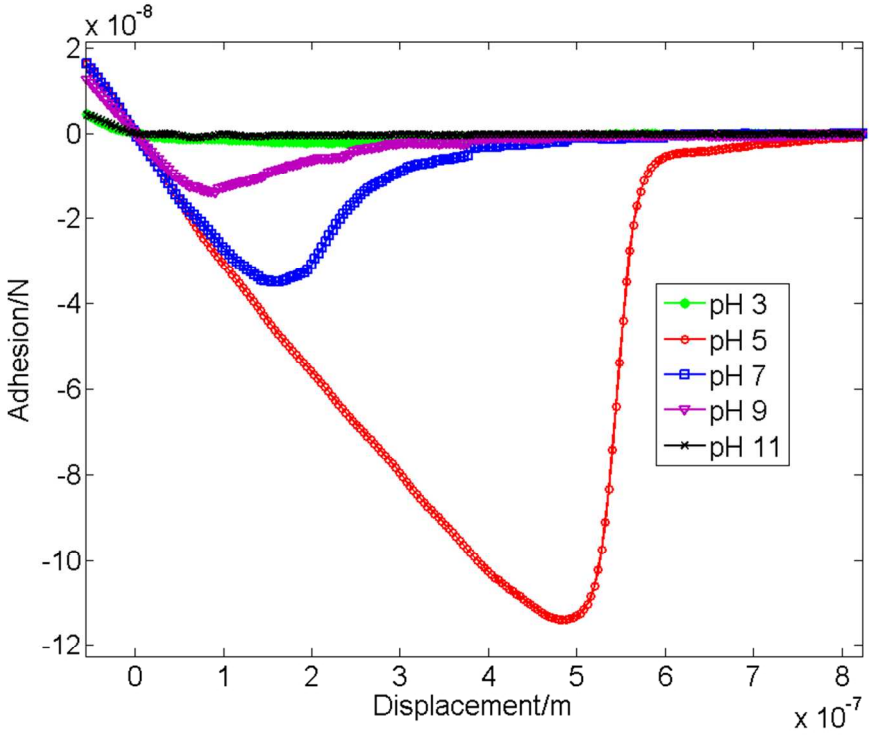

Fig 12(b)
259x196mm (96 x 96 DPI)